Structure, Volume *21*

Supplemental Information

Structural Basis for Eliciting a Cytotoxic Effect in HER2-Overexpressing Cancer Cells via Binding to the Extracellular Domain of HER2

Christian Jost, Johannes Schilling, Rastislav Tamaskovic, Martin Schwill, Annemarie Honegger, and Andreas Plückthun

Inventory of Supplemental Information

Figure S1: Sequence and binding specificity of DARPins relates to Fig. 1
Fig. S1A: (ELISA with monovalent DARPins)
Explanation: ELISA confirm the bispecific binding of the DARPins used in the XTT-assays of Fig. 1
Fig. S1B: (flow cytometry with HER2 monovalent DARPins)
Explanation: Binding competition of DARPins used in the XTT-assays of Fig. 1 on intact cells

Figure S2: Conservation of HER2 domain structures relates to Fig. 2
Fig S2A (overlay of HER2_I on full-length HER2-ECD)
Fig S2B (overlay of HER2_IV on full-length HER2-ECD)
Explanation: Overlays justify the superposition performed in Fig. 3
Fig. S2C (overlays of G3 structures)
Explanation: overlay showing the rigidity of DARPin G3

Figure S3: Sequence comparisons of ErbB domains and of DARPins relates to Fig. 2 and 4
Explanation: Indicates sequence differences between HER1, HER2, HER3, and HER4 sequence differences between DARPins 9.29 and 9.26, epitope and paratope residues.

Figure S4: Linker length of the bivalent DARPins. relates to Fig. 5
Explanation: Illustrates the linker lengths in the different 9_x_G constructs

Table S1. Fitted off-rates of mono- and bivalent DARPins from cells relates to Fig. 1
Explanation: This quantification proves bivalent binding on cells

Table S2. List of the major interaction contacts in the HER2_I/9_29 complex relates to Fig. 2
Explanation: Lists binding interactions for the HER2-I:9_29 complex shown in Fig. 2A-C

Table S3. List of the major interaction contacts in the HER2_IV/G3 complex relates to Fig. 2
Explanation: Lists binding interactions for the HER2-IV:G3 complex shown in Fig. 2D-F

Table S4. List of RMSD(CA) values (Å) of all solved structures. relates to Fig. 3
Explanation: RMSD values justifying the superposition performed in Fig. 5

Supplemental Data

A

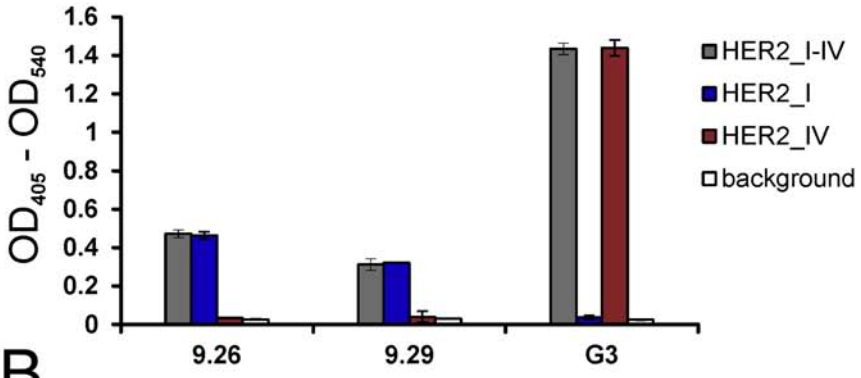

B

>HER2_I

HHHHHHQVCT GTDMKLRLPA SPETHLDMLR HLYQGCQVVQ GNLELTYLPT
DASLSFLQDI QEVQGYVLIA HNQVRQVPLQ RLRIVRGTQL FEDNYALAVL
DNGDPLDNTT PVTGASPGGL RELQLRSLTE ILKGGVLIQR NPQLCYQDTI
LWKDIFHKNN QLALTLIDTD RSRACHPCSP MCKGSRCWGE SSEDCQSLTR
TVA

>HER2_IV

HHHHHHVDCS QFLRGQECVE ECRVLQGLPR EYVNARHCLP CHPECQPQDG
SVTCFGPEAD QCVACAHYKD PPFCVARCPS GVKPDLSYMP IWKFPDEEGA
CQP

>HER2_I-IV

HHHHHHQVCT GTDMKLRLPA SPETHLDMLR HLYQGCQVVQ GNLELTYLPT
NASLSFLQDI QEVQGYVLIA HNQVRQVPLQ RLRIVRGTQL FEDNYALAVL
DNGDPLNNTT PVTGASPGGL RELQLRSLTE ILKGGVLIQR NPQLCYQDTI
LWKDIFHKNN QLALTLIDTN RSRACHPCSP MCKGSRCWGE SSEDCQSLTR
TVCAGGCARC KGPLPTDCCH EQCAAGCTGP KHSDCLACLH FNHSGICELH
CPALVTYNTD TFESMPNPEG RYTFGASCVT ACPYNYLSTD VGSCTLVCPL
HNQEVTAEDG TQRCEKCSKP CARVCYGLGM EHLREVRAVT SANIQEFAGC
KKIFGSLAFL PESFDGDPAS NTAPLQPEQL QVFETLEEIT GYLYISAWPD
SLPDLSVFQN LQVIRGRILH NGAYSLTLQG LGISWLGLRS LRELGSGLAL
IHHNTHLCFV HTVPWDQLFR NPHQALLHTA NRPEDECVGE GLACHQLCAR
GHCWGPGPTQ CVNCSQFLRG QECVEECRVL QGLPREYVNA RHCLPCHPEC
QPQNGSVTCF GPEADQCVAC AHYKDPPFCV ARCPSGVKPD LSYMPIWKFP
DEEGACQPA

C

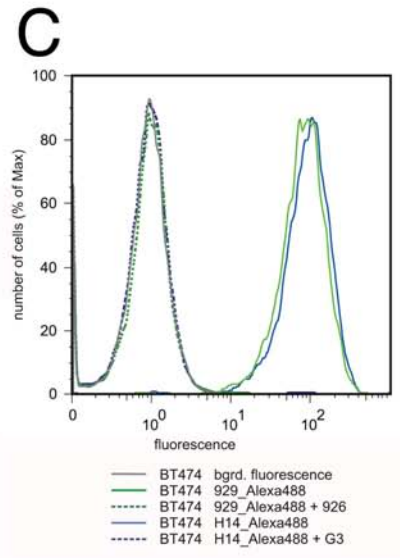

D

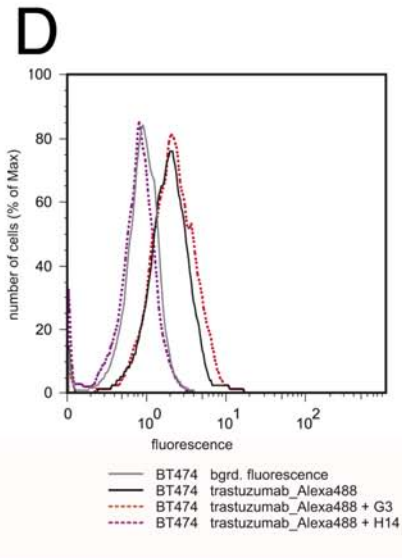

(preceding page) Figure S1, related to Figure 1: Sequence and binding specificity of DARPins

(A) ELISA of HER2 binding DARPins 9_26, 9_29 and G3. The respective DARPins were tested for binding to the immobilized target proteins HER2_I-IV, HER2_I or HER2_IV, respectively. Error bars indicate standard deviation (SD).

(B) Sequence of ELISA targets. HER2_I-IV contains the entire extracellular part of HER2, whereas HER2_I and HER2_IV denote the respective single domains, and the sequences are given underneath. The N-glycosylation sites (highlighted in red) were mutated (N-->D) for crystallization.

(C, D) Competition experiments using flow cytometry with AlexaFluor488-conjugated HER2-binders. BT474 cells were incubated with the respective fluorescently labeled HER2 binder at 100 nM concentration, either without (solid lines) or with (dotted lines) prior preincubation of the cells with the indicated non-labeled competitor at 1 μM concentration. **(C)**, DARPins, **(D)** trastuzumab control.

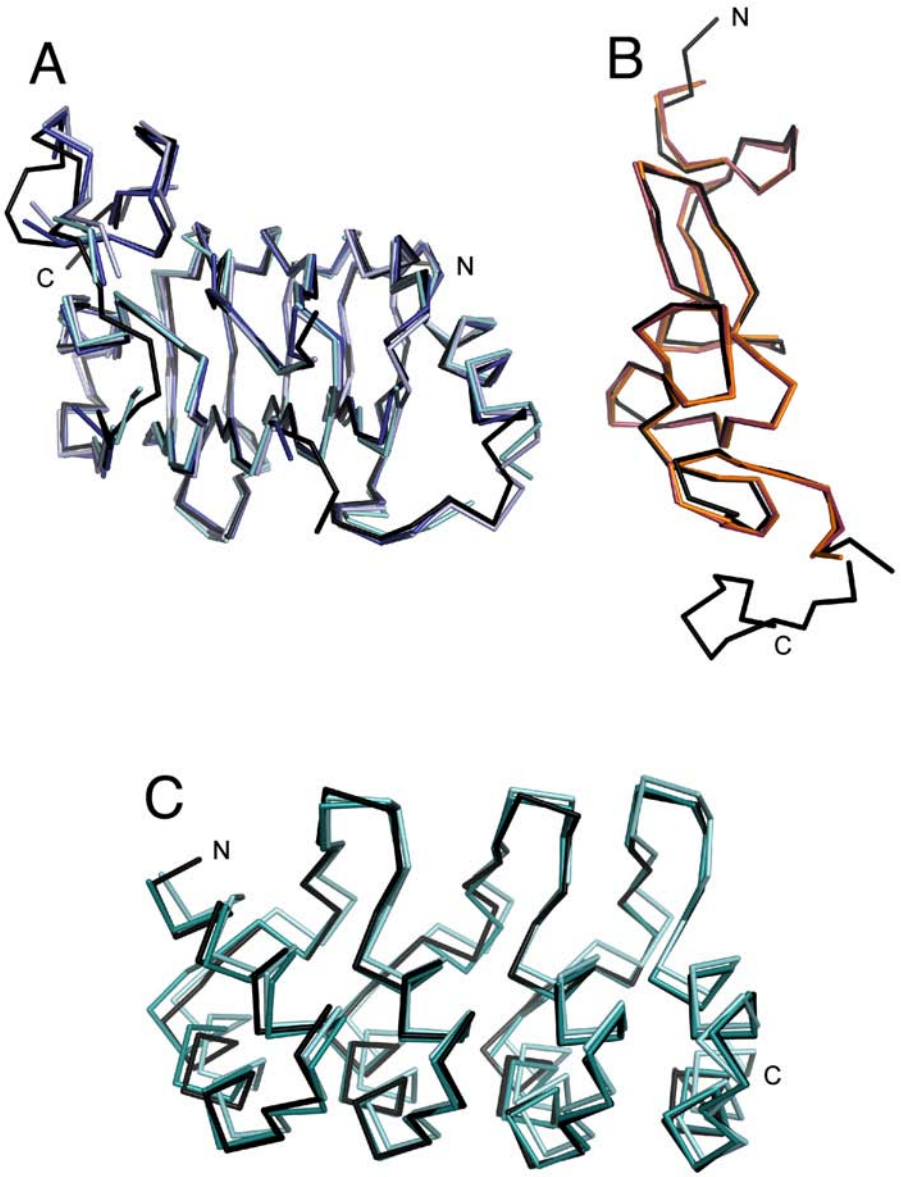

Figure S2, related to Figure 2: Conservation of HER2 domain structures

(A) Overlay of the HER2_I-chains from the two DARPin-complex structures (chain A from HER2_I–9_29 in dark blue; chain A and C from HER2_I–9_26 in cyan and light blue, respectively) with the same domain from HER2_ECD (PDB ID:1N8Z) (black).

(B) Overlay of HER2_IV from the complex structure with DARPin G3 (chain C in orange; chain D in raspberry) with the same domain from HER2_ECD (black). See Table S5 for a complete list of the corresponding RMSD values.

(C) Overlay of the different X-ray structures of DARPin G3, either co-crystallized with HER2-subdomain IV or without target (Zahnd et al., 2007). The chains found in the complex structure (chain A in light blue; chain B in cyan) are very similar to the known structure of uncomplexed G3 (black) (PDB ID:2JAB). See Table S5 for a complete list of the corresponding RMSD values.

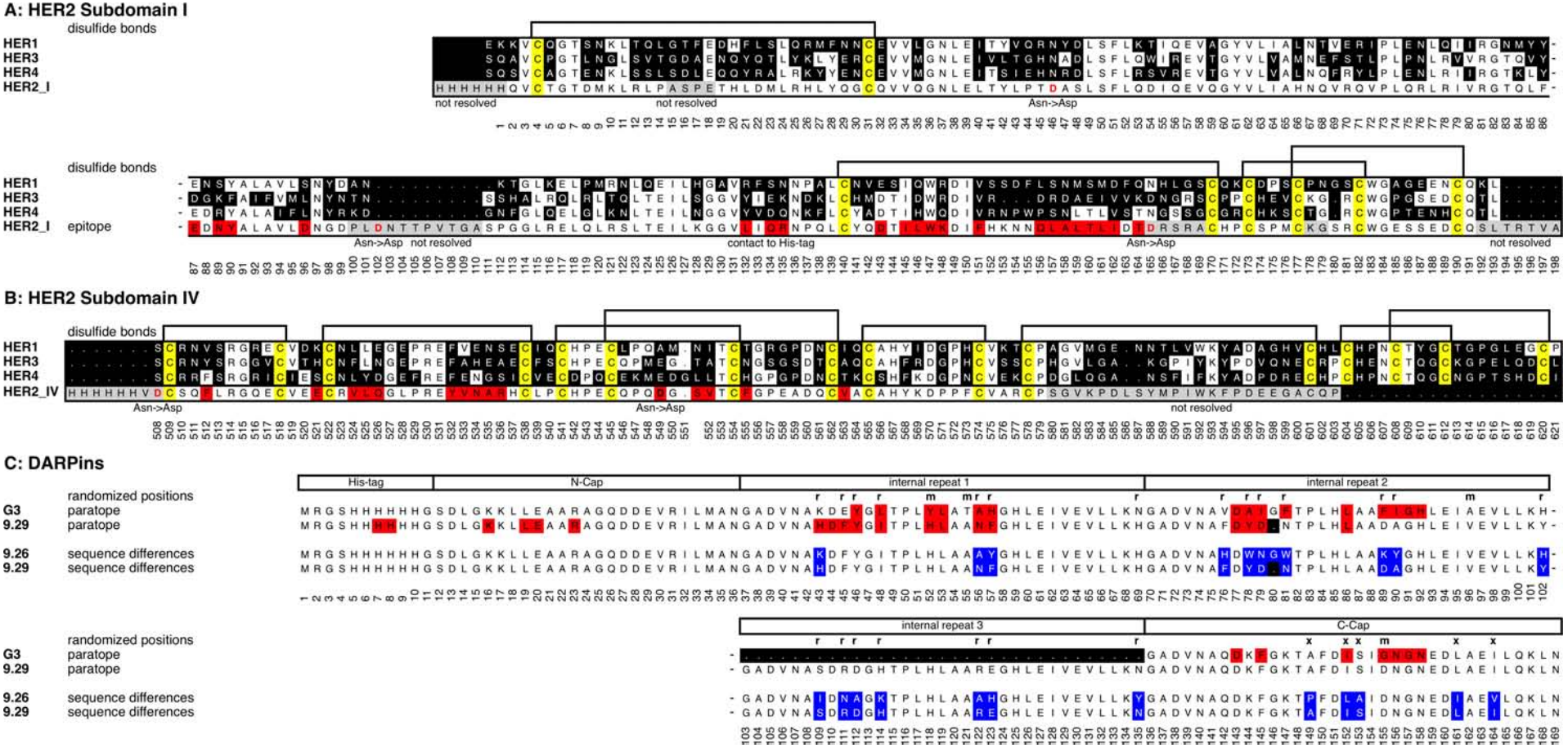
A: HER2 Subdomain I
disulfide bonds
HER1
HER3
HER4
HER2_I
not resolved
not resolved
Asn->Asp
disulfide bonds
HER1
HER3
HER4
HER2_I
epitope
Asn->Asp
not resolved
contact to His-tag
Asn->Asp
not resolved
B: HER2 Subdomain IV
disulfide bonds
HER1
HER3
HER4
HER2_IV
Asn->Asp
Asn->Asp
not resolved
C: DARPins
His-tag
N-Cap
internal repeat 1
internal repeat 2
randomized positions
G3
paratope
9.29
paratope
9.26
sequence differences
9.29
sequence differences
internal repeat 3
C-Cap
randomized positions
G3
paratope
9.29
paratope
9.26
sequence differences
9.29
sequence differences

(preceding page) Figure S3, related to Figures 2 and 4: Sequence comparisons of ErbB domains and of DARPins

(A,B) Sequences of HER2-I and HER2-IV constructs in comparison to the sequences of HER1, HER3 and HER4. Residues in these related sequences that are identical to the HER2 sequence are shown black on white background, sequence differences as white letters on black background, the cysteine residues on yellow background. Subdomain I of HER2 includes the first two interlocked disulfide bonds of the Cys-rich subdomain II .HER2 residues having at least one non-hydrogen atom within 5.0 Å of a non-hydrogen atom of the DARPin are considered part of the epitope and highlighted by a red background. Potential N-linked glycosylation sites were removed by replacing the asparagine by an aspartate residue.

(C) Sequences of DARPins G3, 9_26 and 9_29. DARPin residues having at least one non-hydrogen atom within 5.0 Å of a non-hydrogen atom of HER2 are considered part of the paratope and highlighted by a red background. Sequence differences between 9.26 and 9.29 are shown in white on blue background. "r" indicates positions randomized in the DARPin libraries, "m" mutations acquired by G3 during affinity maturation, improving the K_D from 270 nM to 0.09 nM (Zahnd et al., 2007) and "x" the mutations introduced into the C-cap to improve stability.

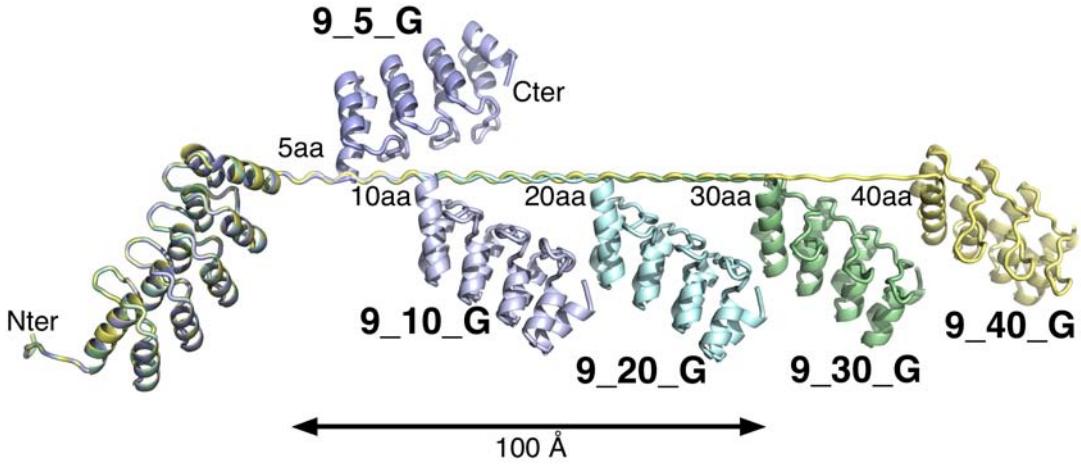

Figure S4, related to Figure 5: Linker length of the bivalent DARPins.

The linker was modeled in β-strand conformation to illustrate the maximal distance that could be bridged by such a linker. In reality, significantly longer linkers will be needed, as the mean end-to-end distance of a flexible polymer scales with the square root of the extended linker length, and the fully extended conformation of a long linker will be sampled very rarely.

Table S1, related to Figure 1. Fitted off-rates of mono- and bivalent DARPins from cells

DARPin	k_{off} (s^{-1})
G3	1.76×10^{-4}
9_20_G	8.13×10^{-5}
G_20_9	4.46×10^{-5}
6_20_G	5.12×10^{-5}
G_20_6	4.80×10^{-5}

Table S2, related to Figure 2. List of the major interaction contacts in the HER2_I/9_29 complex

9_29 interaction residue (repeat module)*			Chain	Interacting atoms (distance in Å, interaction)	HER2_I interaction residue*		Chain
HIS	7	(tag)	A		ARG	135	C
HIS	8	(tag)	A		ARG	135	C
LYS	6	(N-cap)	A	CG-OH (3.86, pi-stacking)	TYR	90	C
LYS	16	(N-cap)	A		LEU	161	C
LYS	16	(N-cap)	A		LEU	32	C
LYS	16	(N-cap)	A	NZ-OE (3.56, H-bond)	GLU	87	C
LYS	16	(N-cap)	A	NZ-OE (2.44, H-bond)	GLU	87	C
GLU	20	(N-cap)	A		ASN	89	C
GLU	20	(N-cap)	A		LEU	159	C
GLU	20	(N-cap)	A		GLU	87	C
GLU	20	(N-cap)	A	OE2-OH (2.51, H-bond)	TYR	90	C
ARG	23	(N-cap)	A		ASN	89	C
ARG	23	(N-cap)	A	NE-O (3.26, H-bond)	LEU	157	C
ARG	23	(N-cap)	A		ALA	158	C
ASP	44	(1)	A		LEU	161	C
ASP	44	(1)	A		LEU	159	C
ASP	44	(1)	A	OD2-N (3.03, H-bond)	THR	160	C
ASP	44	(1)	A		ALA	158	C
PHE	45†	(1)	A	N-O (2.67, H-bond)	THR	160	C
PHE	45†	(1)	A		ILE	162	C
PHE	45†	(1)	A		ASP	143	C
TYR	46†	(1)	A		LYS	148	C
TYR	46†	(1)	A		THR	160	C
TYR	46†	(1)	A	OH-N (3.19, H-bond)	TRP	147	C
TYR	46†	(1)	A		ILE	145	C
ILE	48†	(1)	A		ALA	158	C
LEU	53	(1)	A		LEU	159	C
LEU	53	(1)	A		LEU	157	C
ASN	56†	(1)	A		LEU	157	C
TYR	78†	(2)	A		LYS	148	C
ASP	79†	(2)	A		LYS	148	C

*A cutoff of 4 Å was applied for interactions.
†Amino acids are located in a randomized position of 9_29.

Table S3, related to Figure 2. List of the major interaction contacts in the HER2_IV/G3 complex

G3 interaction residue (repeat module)*			Chain	H-bond (Å)	HER2_IV interaction residue*		Chain
TYR	46†	(1)	A		ASP	49	D
LEU	48†	(1)	A		GLY	50	D
TYR	52‡	(1)	A		LEU	25	D
ALA	56†	(1)	A		LEU	25	D
HIS	57†	(1)	A	ND1-OE (2.90, 3.05)	GLU	21	D
HIS	57†	(1)	A		GLN	26	D
ASP	77	(2)	A		GLY	50	D
ASP	77	(2)	A		SER	51	D
ALA	78†	(2)	A	N-O (2.81)	GLY	50	D
ALA	78†	(2)	A		SER	51	D
ILE	79†	(2)	A		SER	51	D
ILE	79†	(2)	A		PHE	55	D
PHE	81†	(2)	A		PHE	55	D
PHE	89†	(2)	A		VAL	33	D
PHE	89†	(2)	A		CYS	54	D
PHE	89†	(2)	A		VAL	52	D
PHE	89†	(2)	A		TYR	32	D
ILE	90†	(2)	A		VAL	33	D
ILE	90†	(2)	A		PHE	12	D
ILE	90†	(2)	A		VAL	24	D
GLY	91	(2)	A	O-NH (3.14)	ARG	36	D
HIS	92	(2)	A		PHE	12	D
GLY	122‡	C-cap	A	O-ND (3.46)	ASN	34	D
ASN	123	C-cap	A		ASN	34	D
ASN	123	C-cap	A		VAL	33	D
ASN	123	C-cap	A	O-N (3.05)	ALA	35	D
ASN	123	C-cap	A		PHE	55	D
GLY	124	C-cap	A		ASN	34	D
GLY	124	C-cap	A		ALA	35	D
ASN	125	C-cap	A	OD1-N (3.27)	ALA	35	D
TYR	46†	(1)	B		GLY	50	C
TYR	46†	(1)	B		ASP	49	C
LEU	48†	(1)	B		LEU	25	C
LEU	48†	(1)	B		GLY	50	C
TYR	52‡	(1)	B		LEU	25	C
ALA	56†	(1)	B		LEU	25	C
HIS	57†	(1)	B	ND1-OE (2.61, 3.61)	GLU	21	C
HIS	57†	(1)	B		GLN	26	C
ASP	77	(2)	B		GLY	50	C
ASP	77	(2)	B		SER	51	C
ALA	78†	(2)	B	N-O (2.85)	GLY	50	C
ILE	79†	(2)	B		SER	51	C
ILE	79†	(2)	B		VAL	63	C
ILE	79†	(2)	B		PHE	55	C
PHE	81†	(2)	B		PHE	55	C
LEU	86	(2)	B		VAL	52	C
PHE	89†	(2)	B		VAL	33	C
PHE	89†	(2)	B		CYS	54	C
PHE	89†	(2)	B		TYR	32	C
ILE	90†	(2)	B		PHE	12	C
ILE	90†	(2)	B		VAL	33	C
HIS	92	(2)	B		PHE	12	C
PHE	112	C-cap	B		PHE	55	C
GLY	122‡	C-cap	B	O-ND (2.92)	ASN	34	C
ASN	123	C-cap	B		VAL	33	C
ASN	123	C-cap	B		ASN	34	C
ASN	123	C-cap	B	O-N (3.01)	ALA	35	C
GLY	124	C-cap	B		ASN	34	C

*A cutoff of 4 Å was applied for interactions.
† Positions randomized in DARPin library.
‡Amino acids were affinity matured (Zahnd, et al. 2007).

Table S4, related to Figure 3. List of $RMSD_{(CA)}$ values (Å) of all solved structures. The pairwise comparisons were calculated both for the solved structures among each other and in comparison with the respective PDB-entries.

	HER2_I (1N8Z)	HER2_I (9_29_C)	HER2_IV (1N8Z)	HER2_IV (G3_C)	G3 (2JAB)	G3 (G3_A)
HER2_I (9_29_C)	0.491					
HER2_I (9_26_A)	0.810	0.660				
HER2_I (9_26_C)	0.794	0.623				
HER2_IV (G3_C)			0.640			
HER2_IV (G3_D)			0.678	0.242		
G3 (G3_A)					0.645	
G3 (G3_B)					0.525	0.441

Supplemental Experimental Procedures

DARPin nomenclature

The full name of DARPin G3 in the original publication (Zahnd et al., 2007) is H10-2-G3.

ELISA

HER2-domains (200 nM in PBS, 100 µl/well) were immobilized on MaxiSorp plates (Thermo Scientific) by overnight incubation at 4°C. For ELISAs, wells were blocked with 300 µl of PBSTB (PBS, 0.1% Tween-20, 0.2% BSA) for 1 h at room temperature. 50 nM of purified DARPins were incubated with the target domains for 1 h at room temperature, followed by three washing steps with 300 µl of PBSTB. For detection of bound DARPins, an anti RGS-His IgG1 mouse antibody (Qiagen) was added (1:5,000 in PBSTB, 1 h at RT) which recognizes the N-terminal MRGS-His_6 tag of the DARPins, and wells were washed as described above. After incubation with a secondary anti mouse-IgG antibody alkaline phosphatase conjugate (Sigma-Aldrich) (1:10,000 in PBSTB, 1 h at RT), pNPP substrate (Fluka) was added to measure alkaline phosphatase activity.

HER2 subdomains produced in Sf9-cells.

The primary sequences of the HER2 subdomains produced in Sf9-cells are shown in Figure S1B. Note that the N-glycosylation sites (highlighted in red) were N->D-mutated for crystallization.

Crystal structures

The high-affinity binding of DARPin 9_29 to HER2_I is governed by six hydrogen bonds, pi-stacking and extended hydrophobic interactions. Starting from the N-terminus of the DARPin 9_29, 9_29:His8 is involved in pi-stacking interactions with Her2_I:Arg135. Hydrogen bonds between the side chains of 9_29:Lys16 and 9_29:Glu20 and the side chains of Her2_I:Glu87 and Her2_I:Tyr90 further contribute to the binding interface. Side-chain-backbone hydrogen bonds between 9_29 residues Arg23, Asp44 and Tyr46 and Her2_I residues Leu157, Thr160 and Trp147, and backbone-backbone hydrogen bonds between 9_29:Phe45 and Her2_I:Thr160 complete the vast hydrogen bonding network. 9_29 residues Lys16, Glu20 and Arg23 are not only involved in hydrogen bonds, but also contact HER2_I residues Leu132, Tyr90, Leu161 and Leu159 via hydrophobic interactions. The first internal repeat of 9_29 employs Phe45, Tyr46 and Ile48 and Leu53 in binding to a hydrophobic depression on HER2_I, which is formed by HER2_I residues Trp147, Thr160, Ile162, Leu161, Leu159, Leu157 and Lys148. Asn56 from the first and Tyr78 and Asp79 from the second internal repeat of 9_29 bind the protruding HER2_I residues Leu157 and Lys148 via hydrophobic interactions. The C-terminal part of 9_29 does not contribute to the interaction with HER2_I.

The 2 complexes in the asymmetric unit of the G3+HER2_IV structure possess practically identical interactions. Therefore, only the complex formed between chain A of G3 and chain D of HER2_IV will be described. Similar to the 9_29+HER2_I complex, the G3+HER2_IV complex contains six hydrogen bonds and extended hydrophobic interactions, which are responsible for the low picomolar affinity of G3. Starting from the N-terminus of the DARPin G3, G3:Tyr46 and G3:Leu48 bind via hydrophobic interactions

to protruding residues Asp49 and Gly50 on HER2_IV, whereas G3:Leu48 and G3:Tyr52 reach into a small hydrophobic groove on HER2_IV formed by Gly50 and Leu25. G3:Ala56 contacts HER2_IV:Leu25 through a hydrophobic interaction. G3:His57 on the other hand contributes the first hydrogen bond with HER2_IV:Glu21 to the interface. A backbone-backbone hydrogen bond and hydrophobic interactions between G3:Ala78 and HER2_IV:Gly50 are followed by hydrophobic interactions between G3 residues Ile79 and Phe81, which bind to a surface exposed hydrophobic patch formed by HER2_IV residues Ser51, Val52 and Phe55. G3:Phe89 perfectly reaches into a semi-circular hydrophobic depression involving Val52, Val24, Val33, Tyr32 and Phe55 on HER2_IV. Ile90 on G3 binds to an adjacent hydrophobic patch formed by HER2_IV residues Val24, Val33 and Phe12. These interactions are followed by hydrogen bonds between the backbone of G3 residues Gly91 and Gly122 with side chains of residues Arg36 and Asn34 on HER2_IV. The backbone-backbone hydrogen bond between G3:Asn123 and HER2_IV:Ala35 and the side-chain-backbone hydrogen bond between G3:Asn125 and HER2_IV:Ala35 complete the vast interaction network between G3 and HER2_IV.

Although G3 possesses only two internal repeats, the perfectly matching hydrophobic and hydrogen bonding interactions account for its extremely high affinity.

Certain residues in the 9_29/HER2_I and G3/HER2_IV complex structures at termini or connecting loops are flexible and therefore not visible in the electron density. In addition, some residues for which the backbone was clearly visible in the electron density, but side chains were partly or fully unresolved in the structure, were built as Alanines and are listed in Table S4.

Interestingly, electron density for HER2_IV is clearly visible for the stretch complexed with DARPin G3. It starts at residue 9 and suddenly becomes untraceable after residue 79 (in chain C; 78 in chain D). The resolved structure of Domains IV in complex with G3 compares very well with Domain IV from full length ECD (PDB ID: 1N8Z) (see Table S5 for $RMSD_{CA}$-values and Fig. S2*B* for overlays of the protein backbones).

The quality of the 9_26/HER2_I structure at a resolution of 3.25 Å is lower than the quality of the aforementioned two structures. Large parts of both, the DARPin 9_26 and Domain I, are unresolved in the structure. Affected residues are listed in Table S4. Interestingly, different parts of 9_26 are resolved in chain B and D and therefore complement each other.

Molecular modeling

To assess conformational differences between different HER2 domain I (HER2_I) structures, HER2 structures 1N8Y, 1N8Z, 1S78, 2A91, 3BE1, 3H3B, 3MZW and 3N85 were aligned by least-squares superposition of the Cα coordinates of residues 21-96 and 116-152 onto the aligned HER2_I-DARPin complexes.

In the structures HER2_I:9_29 and HER2_I:9_26, several HER2_I positions near the N-terminus, in loop 99-114 and near the C-terminus of the domain are missing. In a composite model, the majority of the residues was taken from structure 3N85, which covers the HER2 structure from residue 2 to 621, the last disulfide-linked Cys of domain IV. The missing loop residues were patched from structure 3H3B; the DARPin binding epitopes were patched from the structures of the DARPin complexes. Missing residues in positions 249-253 of 3N85 were patched in a similar manner. The coordinates of an unpublished X-ray structure of unliganded DARPin 9_26 were used to provide the missing residues of the DARPin in the complex. However, for further modeling, the 9_29 complex was used, since the two DARPins recognize the same epitope. The DARPin G3–HER2_IV complex was fitted to domain IV of structure 3N85 by superposition of residues 510 to 563.

All models were built using the Homology module of InsightII (Accelrys, San Diego) to assign the coordinates from the aligned templates to the complete sequence, the "Discover" module to locally energy minimize the sites where different templates were spliced, and „Rosetta 3.4“ (www.rosettacommons.org) for constrained relaxation of the final model.

The best-resolved tethered structures of HER1, HER3 and HER4 were superimposed by a least-squares fit of domain III to assess the divergence. To build a model of the hypothetical tethered conformation of HER2, each domain of HER2 was superimposed separately on the corresponding domain of the template structure of HER4 (2AHX). HER2_I was superimposed on HER4_I by least-squares superposition of the Cα atoms of residues A32-A96 and A116-A141 of HER2 on A31-A95 and A106-A131 of HER4 (RSMD 0.65 Å). Domain II of a second copy of HER2 was superimposed on domain II of HER4 by least-squares superposition of the Cα atoms of residues A206-A247 and A268-A282 of HER2 on A196-A237 and A258-272 of HER4 (RSMD 0.56 Å). Domain III of HER2 was superimposed on domain III of HER4 by least-squares superposition of the Cα atoms of residues A321-A324, A337-A356, A371-A414 and A429-A454 of a third copy of HER2 on residues A309-A312, A325-A344, A359-A402 and A417-A442 HER4 (RSMD 0.55 Å). Domain IV of HER2 was superimposed on domain IV of HER4 by least-squares superposition of the Cα atoms of residues A510-A546 and A555-A579 of a fourth copy of HER2 on residues A498-A534 and A544-A568 of erbB4 (RMSD 0.57 Å) Coordinates were assigned to the model from the properly oriented HER2 domain templates using the Homology module of InsightII and the joining regions as well as the tethering loops were extensively energy-minimized, while the domains themselves were constrained to their initial conformation. Binding partners DARPin 9_29 and DARPin G3 were transferred in the correct relative orientation from the template model to the final model.

For the model of the HER2 homodimer, individual domains of HER2 were superimposed on the corresponding domains of the HER4 homodimer structure 3U7U. This was unproblematic for domains I, III, and IV. For domain II, however, no good fit of the entire domain could be found, and therefore, the N-

and C-terminal half of the domain were fitted separately, the conformations of the tethering loop adjusted, and the entire domain minimized, constraining only the positions of the disulfide-linked Cys residues.

To include the transmembrane (TM) domain and the kinase domain into the models, extracellular domain, NMR models of the TM domain (PDB entry 2JWA) and kinase structures (PDB entry 3PP0 for the active kinase dimer, 3RCD for the inactive kinase) were oriented in space taking electron micrographs from Zhang et al. (2012) as a guide. Seven residues between the last disulfide bridge of HER2_IV and the start of the transmembrane helix and 30 residues between TM domain and the kinase were treated as flexible to connect the domains. Local minimization of flexible regions and patched loops using the „Discover" module of InsightII were followed by constrained relaxation using Rosetta.

To explore the conformations that would allow crosslinking with the shortest (five-amino-acid) linker constructs, the models with attached unlinked DARPins were cut at the chosen pivot point and rotations around this pivot point were explored to identify conformations that would bring the termini into a distance compatible with such a short linker without any overlap of the proteins. Fig. 6 in the main paper shows two such solutions for bispecific DARPin 9_5_G.

It should be pointed out that the bispecific DARPin 9_5_G can also link a HER2 molecule in the open conformation with one in the tethered conformation, leading to the same conclusions as shown in Fig. 6. In principle, more distorted conformations of HER2 are conceivable, but there is currently no evidence for those.

In the paper, we mainly discussed the more active 9_x_G orientation of the bivalent DARPins. In this orientation, short linkers would pull down subdomain I of the HER2 monomers in such a way that the dimerization interface is obstructed by the membrane and by the second HER2 monomer kept in an orientation unsuitable for dimerization with the first monomer. This obstruction by the second HER2 monomer, especially in the context of long daisy-chains of HER2 molecules, may become the main mechanism of inhibition in constructs with linkers that are too long to significantly tilt the ECD. Due to the spatial arrangement of the DARPin termini in the HER2 complex, the less active G_x_9 constructs would tilt the HER2-ECD sideways, in an orientation less suitable to obstruct the dimer interface. The resulting side-by-side arrangement of the HER2-ECDs is also less effective at obstructing the dimerization interface and preventing activating dimerization with an additional HER2 monomer in constructs with longer linkers.

Supplemental References

Zahnd, C., Wyler, E., Schwenk, J. M., Steiner, D., Lawrence, M. C., McKern, N. M., Pecorari, F., Ward, C. W., Joos, T. O., and Plückthun, A. (2007). A designed ankyrin repeat protein evolved to picomolar affinity to HER2. J. Mol. Biol. *369*, 1015-1028.

Zhang Q., Park E., Kani K., and Landgraf R. (2012) Functional isolation of activated and unilaterally phosphorylated heterodimers of ERBB2 and ERBB3 as scaffolds in ligand-dependent signaling. Proc Natl Acad Sci U S A *109*,13237-13242.